RADAR

MST and ST Radars and Wind Profilers

R F Woodman, Instituto Geofísico del Perú, Lima, Peru

Short History and Definitions

MST stands for mesosphere–stratosphere–troposphere and qualifies VHF (very high frequency) radar systems capable of observing all these regions of the atmosphere. The technique was developed and used for the first time in the early 1970s at the Jicamarca Radio Observatory, an incoherent-scatter facility of the Instituto Geofísico del Perú, located near Lima, Peru (see **Figure 1**). The name that is now used was coined a few years later on the occasion of the US National Academy of Science workshop on the Use of Radar for Atmospheric Research in the 1980s, held in Salt Lake City, Utah, in 1978.

To reach mesospheric altitudes, the system must normally have a very large antenna (or antennas) and a powerful transmitter. In the case of the Jicamarca radar, the antenna is a square array of dipoles 300 m on a side, and the transmitter has more than 2 MW of peak power. After the success of the Jicamarca radar in obtaining radar echoes from these mid-atmospheric altitudes, other radars were built specifically for this purpose: the SOUSY radar in the Harz, Germany; the Poker Flat radar in Alaska (no longer in operation); the MU radar in Shigaraki, Japan; and the Gadanki radar in Tirupati, India. The VHF EISCAT radar, in Tromsø, Norway, although built mainly for incoherent-scatter ionospheric studies, should also be included in the list.

To qualify as an MST radar, the system has to be capable of obtaining echoes from the mesosphere. This requirement limits the frequency range of these radars to the lower frequencies of the VHF band, i.e., between 30 and 300 MHz. Smaller radars, using the same principles and techniques but capable of reaching only the stratosphere and troposphere, are called ST radars. Here we can cite as an example the NOAA Tropical Pacific Profiler Network in the equatorial Pacific, and the wind profiler network in central United States as important multiple radar installations that qualify as such. These, and even smaller systems capable of observing only the troposphere, are also called wind profilers, because of their main use as operational radars dedicated to measuring the winds aloft in a continuous manner. At these lower altitudes it is possible to use frequencies higher than VHF frequencies. Nowadays, many radars designed for other purposes, including operational air traffic, meteorological Doppler radars, and ionospheric incoherent-scatter radars, are also used as ST radars.

Figure 1 Panoramic view of the Jicamarca Radio Observatory and its 300 m × 300 m antenna array. The building houses a powerful transmitter with approximately 3 MW of peak power. It was the first MST radar and it is still the most powerful.

At polar and near-polar latitudes a very special mesospheric geophysical phenomenon manifests itself with a greatly enhanced radar reflectivity and permits the use of smaller VHF systems. These smaller radars, when operated at these latitudes, could also be classified as MST radars. The Mobile-SOUSY radar operating in Svalbard, Norway, the Peruvian radar installed at its Machu-Picchu Antarctic station, and the Cornell University mobile radar (CUPRI) belong to this category. The list is not exhaustive and it includes only some of the early systems. The high-reflectivity phenomenon was discovered by the Poker Flat MST radar and is referred to as PMSE, for polar mesospheric summer echoes, with occurrence limited to the summer months.

Lastly, we are now seeing the proliferation of even smaller radars that use the same techniques but are limited to study of the lower troposphere; these are referred to as boundary layer radars (BLRs).

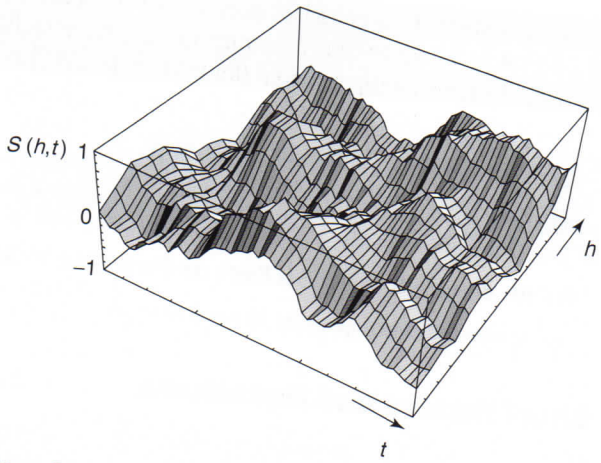

Figure 2 Schematic representation of the radar received signal, $S_h(t) \equiv S(h, t)$, as a two-dimensional random process. The process is sampled at the altitude of the echoing region, h, and a time t, corresponding to the time of the transmitted pulse. The process is complex. Here we are representing only the real (or imaginary) component.

The Basic Technique

The MST radar technique involves the illumination of a target with a pulsed electromagnetic (EM) wave. The target, in this case the clear atmosphere, scatters a very small fraction of the energy of the wave in all directions, including the direction to the receiving antenna, which in most cases is the same antenna used for transmission. We should underline here 'clear atmosphere' to differentiate the technique from meteorological radars that depend on hydrometeors (rain, snow, hail) to act as targets. At reception, the returned echoes are amplified and discriminated in range by sampling them at different delays with respect to the time at which the transmitted pulse was emitted, taking advantage of the finite speed of propagation of the probing wave (the speed of light). The sampled signal forms a two-dimensional discretely sampled complex random-process $S(h, t)$, such as the one depicted in **Figure 2**. One of the dimensions is the sample delay, or range h, and the other is the discrete time t corresponding to the emission of the transmitter pulse. Given the practical statistical independence of the process for different h's, it is preferable to think of the process as multiple random processes in t, $S_h(t)$, one for each h.

The complex nature of $S_h(t)$ is a consequence of the coherent nature of the detection scheme used. The magnitude of $S_h(t)$ is proportional to the amplitude of the received radio signal, and its phase is that of the received signal with respect to the transmitted one. In practice, the signal is obtained and represented by its real and imaginary components.

The received signals are digitized and fed to a digital processing system. There they are grouped and statistically processed as multiple independent time-series, one for each range ($h = 1, 2, \ldots, N$). The statistical parameters obtained for each series are related to the properties of interest corresponding to each particular range, h, as discussed in the following sections.

One characteristic of the MST or ST echoes is the slowness of the process as compared to the typical pulse repetition rate, i.e., the sampling time interval. The corresponding interpulse period is determined by the maximum altitude (delay) of the region under study. This period is of the order of a fraction of a millisecond, whereas the characteristic time of the process is of the order of a second or more. This permits the coherent addition of many samples of almost identical value before any further processing is done. This is a common pre-processing scheme in all MST radars and has a twofold advantage: it enhances the signal-to-noise ratio of the signal prior to its later processing and, more importantly, it reduces the digital statistical-processing speed requirements by about two orders of magnitude.

Underlying Principles

The MST radar technique is based on the scattering properties of minute fluctuations in index of refraction at the altitudes of interest. At tropospheric and stratospheric altitudes, these fluctuations in refractive index come about as a consequence of fluctuations in the density of the medium. At mesospheric altitudes, the medium is ionized and it is the density of free electrons that determines its index of refraction. Hence, the scattering is produced by fluctuations in

electron density. In all cases, the fluctuations in index of refraction, small as they are, must be enhanced well above the ever-existing thermal fluctuation level. This enhancement is usually produced directly or indirectly by turbulence.

At tropospheric heights the MST radar technique, although it does not exclude fluctuations produced by the presence of hydrometeors, depends mainly on clear-air fluctuations of the dielectric properties of the medium. This dependence on clear-air fluctuations differentiates the MST or ST techniques from the older and better-known meteorological radars, which do depend on the existence of hydrometeors. The fact that MST radar technique does not require the presence of hydrometeors extends the usefulness of the technique by permitting continuous 24-hour observations of the stratosphere and troposphere. At mesospheric altitudes the MST radar technique is useful mainly during (mesospheric) daytime hours when free electrons exist. At polar latitudes the time is extended during the summer almost to a full day, depending on the latitude.

Fluctuations in the index of refraction in the atmosphere are of a stochastic nature; consequently, the radar echoes they produce are also stochastic. Both have to be characterized statistically. If we denote the fluctuating component (zero mean) of the index of refraction of the medium at position $\mathbf{x}$ (vectors are represented by bold letters) and time t by $n(\mathbf{x}, t)$, an important statistical property of the medium is given by its un-normalized space–time autocorrelation function, $\rho(\mathbf{r}, \tau)$, defined in eqn [1].

$$\rho(\mathbf{r}, \tau) = \langle n(\mathbf{x}, t)\, n(\mathbf{x} + \mathbf{r}, t + \tau) \rangle \qquad [1]$$

Here, $n(\mathbf{x} + \mathbf{r}, t + \tau)$ denotes the fluctuation in index of refraction measured at a displaced position $\mathbf{r}$ and time lag τ. Both displacements refer to the point, $\mathbf{x}$, and time, t, where $n(\mathbf{x}, t)$ is initially measured. The angle brackets represent an ensemble average. We have assumed that the medium is homogeneous within a large space around $\mathbf{x}$, and stationary within an observational time centered around t, hence the independence of $\rho(\mathbf{r}, \tau)$ on these variables. The statistical properties of the received signal, $S_h(t)$, as defined before, scattered from a region of range h, are characterized in turn by its temporal correlation function $C_h(\tau)$. Furthermore, it can be shown that these two statistical averages are, under simplifying assumptions, related as in eqn [2].

$$C_h(\tau) \equiv \langle S_h(t) S_h^*(t + \tau) \rangle = A \int \rho_h(\mathbf{r}, \tau)\, \mathrm{e}^{-\mathrm{j}\mathbf{k}\cdot\mathbf{r}}\, \mathrm{d}\mathbf{r} \qquad [2]$$

where A is a constant of proportionality that depends on the radar system parameters, including – among others – the radar power and its antenna gain. The vector $\mathbf{k}$ is called the scattering Bragg wave vector and stands for the vector difference $\mathbf{k}_\mathrm{i} - \mathbf{k}_\mathrm{s}$. The terms $\mathbf{k}_\mathrm{i}$ and $\mathbf{k}_\mathrm{s}$ stand, in turn, for the incident and scattered electromagnetic wave vectors, respectively. Note that we have relaxed the assumption of homogeneity of the medium, allowing $\rho_h(\mathbf{r}, \tau)$ to vary slowly as a function of the range h.

In most MST radar systems the transmitter and receiving antenna are in the same place. Then, the incident and the scattered wave vectors are aligned with the line of sight but with opposite signs. In such a case the Bragg vector $\mathbf{k}$ is equal to $2\mathbf{k}_\mathrm{i}$ and has a magnitude equal to twice the wavenumber corresponding to the radar frequency, ω, i.e., $k = 2 \times 2\pi/\lambda = 2\omega/c$, where c is the speed of light and λ is the radar wavelength.

The potential of the MST radar technique, as well as of other radars used to observe the atmosphere, is based on the simple functional relationship of eqn [2]. Note that the integral operation on $\rho_h(\mathbf{r}, \tau)$ is its three-dimensional Fourier transform evaluated at a single wave vector $\mathbf{k}$. The first conclusion we can derive from eqn [2] is that the radar is sensitive only to one of the Fourier components of $\rho_h(\mathbf{r}, \tau)$, that corresponding to $\mathbf{k}$, and, hence, on the basis of the Wiener–Khinchin theorem, to the same Fourier component of the random fluctuations $n(\mathbf{x}, t)$. The fluctuations represented by $n(\mathbf{x}, t)$ can be thought of as the Fourier superposition of many sinusoids of different wavelengths. However, the radar will see only one component of the fluctuations, $\tilde{n}(\mathbf{k}, t)$, i.e., the one with a wavelength equal to half the wavelength of the radar and a direction aligned with the line of sight (in the backscatter case) of the radar. Furthermore, the power of the echo returns, given by $C_h(0)$, is proportional to the power spectral density of this fluctuation component, $\langle \tilde{n}(\mathbf{k}, t)^2 \rangle$. Additionally, the temporal dynamics of $C_h(\tau)$ depends on the dynamics of this spatial Fourier component of the fluctuations.

We have characterized above the statistical properties of the received signals by the autocorrelation function, $C_h(\tau)$, of the time-series they generate. They can also be characterized by their frequency power spectra, $F_h(\omega)$, since this is the temporal Fourier transform of $C_h(\tau)$ (eqn [3]).

$$F_h(\omega) = \frac{1}{2\pi} \int C_h(\tau)\, \mathrm{e}^{-\mathrm{j}\omega\tau}\, \mathrm{d}\tau \qquad [3]$$

In fact, in most MST radar processing systems, the frequency spectrum is evaluated directly from the series it characterizes, taking advantage of the speed of the fast Fourier transform (FFT) algorithm. The frequency spectrum is also preferred by many users

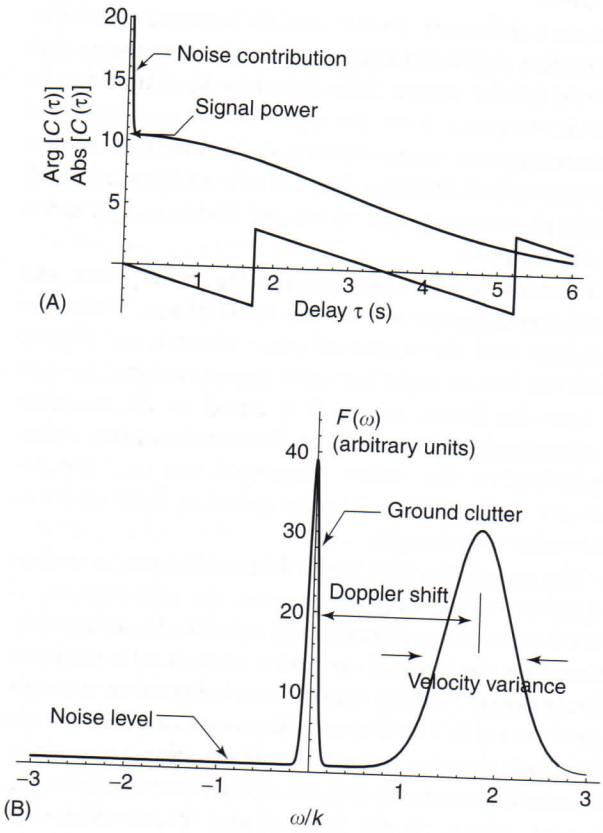

Figure 3 Statistical properties of the time series at a given altitude, h: (A) its complex, amplitude and phase, temporal autocorrelation function $C_h(\tau)$; (B) its corresponding frequency spectrum, $F_h(\omega)$.

of the technique for discussing the physical meaning of the observations. **Figure 3** shows schematically the typical shape of these two functions, $C_h(\tau)$ and $F_h(\omega)$. We will discuss later the physical significance of their characterizing parameters.

On the Origin of the Scattering Fluctuations

To interpret the MST radar results we need a model of the physical mechanisms responsible for the fluctuations in index of refraction that are responsible for the radar echoes. In most cases, the small-scale fluctuations are produced by turbulent processes. Acoustic waves can also produce scattering fluctuations, but only if excited significantly by artificial means.

Turbulence occurs in the atmosphere as a consequence of static or dynamic instabilities. Under the presence of a gradient in the undisturbed index of refraction, turbulence will mix parcels of high index into regions of low index of refraction, and vice versa. Once these primary fluctuations are formed, smaller secondary fluctuations are produced as a consequence of smaller-scale mixing working on the larger scale fluctuating gradients. In the case of the neutral atmosphere the index of refraction depends on the neutral density, which for a given pressure depends on temperature.

The required original gradient in index of refraction has to deviate from that produced by the normal static exponential vertical pressure gradient of the atmosphere produced by gravity. One actually requires an initial gradient in potential temperature (temperature at a constant reference pressure). Potential temperature behaves as a passive scalar, i.e., stays invariant in a Lagrangian description of the turbulent motions, despite the presence of the exponential static pressure gradient; thus it fluctuates as any other passive scalar as a consequence of turbulence mixing.

In the mesosphere, the index of refraction depends on the electron density. For turbulence to produce the necessary fluctuations, we need a gradient in this density, or more properly in the potential electron density (i.e., electron density at a given reference pressure). The behavior of electron density as a passive scalar can be questioned because of production and recombination processes, but these can be partially ignored given their relatively large characteristic times at these altitudes.

Apart from the fluctuations produced directly by turbulent mixing, other indirect effects may also produce scattering structures. Here we need to consider that turbulence in the atmosphere, with exception of that produced by tropospheric thermal convection processes, is stratified. This is a consequence of the fact that dynamic instabilities produce turbulence only at altitudes where the vertical shear of horizontal velocities exceeds a critical level. Thus, the transition region from turbulent to nonturbulent can be very thin, producing essential discontinuities in the vertical profile of index of refraction with a large horizontal extent. If the discontinuity has a horizontal dimension larger than a Fresnel radius, it can produce a partial reflecting structure with almost specular properties. Alternatively, these structures can be incorporated in the formalism expressed by eqns [1] and [2] above as very flat, disklike, local correlation functions to which corresponds an almost unidirectional spatial wave vector ($\mathbf{k}$) spectrum. We then speak of 'aspect-sensitive' structures with enhanced scattering properties in the vertical direction.

Furthermore, the transition from turbulent to nonturbulent is a region where the initial vertical shear is concentrated. This shear will take an initially isotropic blob and deform it into an elliptical shape, also producing almost horizontal aspect-sensitive structures with similar scattering effects.

The existence of these aspect-sensitive structures complicates the interpretation of the radial velocities measured by the radar since it effectively introduces a bias in the effective pointing direction of the antenna beam. On the other hand, the enhancement in reflectivity produced by these aspect-sensitive structures is used by some ST techniques, by pointing only in the vertical direction, to reduce the required power and/or antenna size while maintaining sufficient sensitivity.

Physical Interpretation of the Radar Echo Characteristics

The frequency spectrum $F_b(\omega)$ of the radar echo returns is usually a bell-shaped function, especially when the radar has sufficient altitude resolution to sample a locally homogeneous region. As such, the spectrum can be well characterized by its first three moments, i.e., its total power or area under the spectrum, its displacement with respect to zero frequency (transmitter frequency), and its width. The contributions of noise and ground clutter, which are always present, have to be subtracted before the analysis.

According to the previous discussion, the total power, $C_b(0) = \int F_b(\omega)\,\mathrm{d}\omega$, is proportional to $\langle \tilde{n}(\mathbf{k}, t)^2 \rangle$, i.e., the spatial spectral power density at wave vector $\mathbf{k}$, and is a proxy of the total fluctuation power $\langle n(\mathbf{x}, t)^2 \rangle$. In fact, under the assumption that the fluctuations are a consequence of turbulent mixing, turbulence theory allows us to infer the latter from the former. We need only to assume $\mathbf{k}$ to be within the inertial subrange of turbulence, i.e., a known spectral shape, and have an estimate of the outer scale, which in many cases can be obtained from the measurements themselves (e.g., layer thickness). Thus the technique allows us to obtain the altitude and temporal distribution of turbulence intensity in the atmosphere. Therefore, the MST power measurements have been used to determine the morphology of turbulence in the atmosphere. Under the assumption of turbulent mixing, MST radar measurements have also been used to estimate turbulent diffusivity and the energy dissipation rate at different altitudes. Regions of high aspect sensitivity can be discriminated by looking off-vertical or with interferometer techniques (see below). Aspect sensitivity can be used, at least in a qualitative fashion, as an indication of the presence of anisotropic turbulence or as an indication of sharp horizontally stratified structures in the index of refraction such as the ones discussed above.

The second characteristic parameter of the frequency spectrum is the displacement of the 'center' of the spectrum with respect to zero frequency (i.e., the transmitter frequency). As intuitively expected, this is a Doppler displacement and is related to the radial velocity of the target. We will show next that this is indeed the case.

Density, and hence dielectric, fluctuations at the scale sizes of interest have two main modes of dynamical behavior – acoustic and diffusive – depending on whether or not there are pressure fluctuations associated with them. Acoustic fluctuations propagate at the speed of sound; diffusive fluctuations do not propagate, they move with the bulk motion of the medium in which they are imbedded. Turbulence-induced fluctuations are diffusive and therefore can be used as tracers of the bulk motions of the atmosphere. Acoustic fluctuations are also capable of scattering if excited at a sufficiently high level. They are the artificially introduced tracers of the radio acoustic sounding system (RASS) technique, which we will briefly mention later.

If a time-varying random fluctuation field does not show any preferred direction with respect to an observer, there is no relative velocity between the observer and the medium. In this case the corresponding space–time autocorrelation function is symmetric under a direction interchange, i.e., $\rho_o(\mathbf{r}, \tau) = \rho_o(-\mathbf{r}, \tau)$. A radar observing from this frame of reference will obtain a real and symmetric spectrum $F_o(\omega) = F_o(-\omega)$. If the same medium moves with velocity $\mathbf{v}$ with respect to the same observing radar, then $\rho(\mathbf{r}, \tau) = \rho_o(\mathbf{r} - \mathbf{v}\tau, \tau)$. It can be shown using eqns [2] and [3] above that the resulting spectrum would then be given by eqn [4].

$$F(\omega) = F_o(\omega - \mathbf{k} \cdot \mathbf{v}) \qquad [4]$$

This is the Doppler effect and means that the point of symmetry of the spectrum would be shifted by a frequency $\Omega = \mathbf{k} \cdot \mathbf{v}$, proportional to the velocity of the medium, $\mathbf{v}$, projected along the Bragg wave vector, $\mathbf{k}$. Since the first moment of the symmetric spectrum $F_o(\omega)$ is zero, the first moment of the displaced spectrum, $F(\omega)$, is given by the displacement $\Omega = \mathbf{k} \cdot \mathbf{v}$. In practice, owing to deviations from medium homogeneity within the scattering volume, one may find that there is no perfect center of symmetry for either $F(\omega)$ or $F_o(\omega)$. Nevertheless, one can always find the first moment and use it as a measure of the (projected) velocity of the medium.

Backscatter radar measures the medium vector velocity component along the line of sight of the radar, at all ranges. **Figure 4** shows an example of a spectrum profile obtained with the Arecibo, Puerto Rico, 430 MHz radar in ST mode. The radial velocity profile can be practically read directly from the graph. By using at least three different and non-coplanar pointing

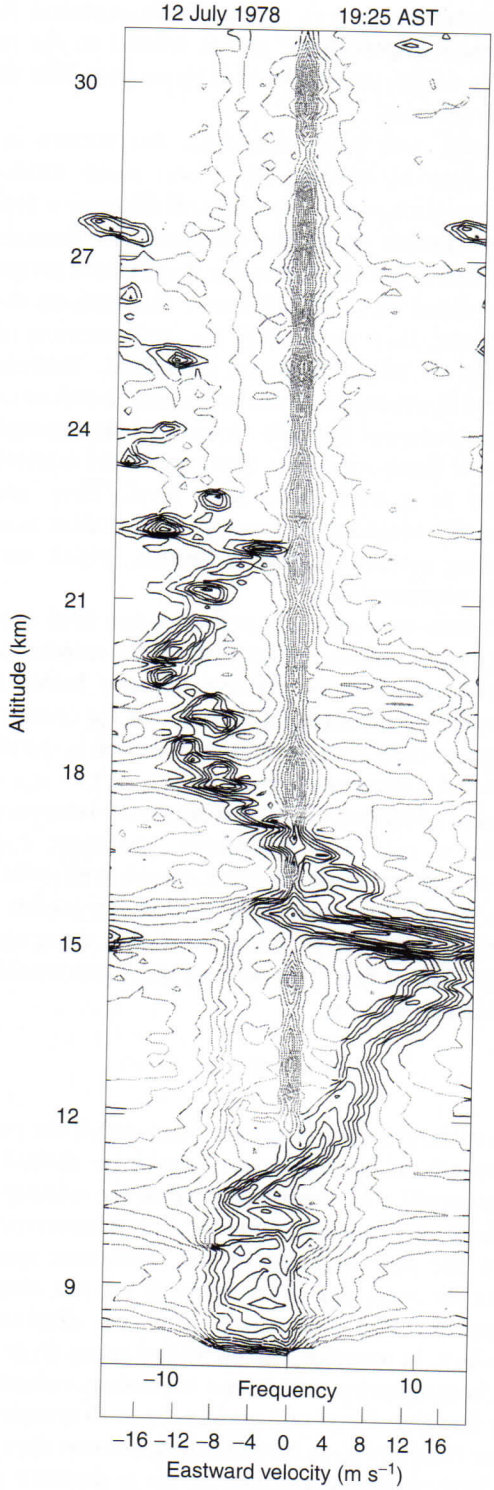

Figure 4 Typical raw statistical data obtained every minute by the 430 MHz radar of the Arecibo Observatory operating in a ST mode. The zenith angle for this observation was 15°. Contours are drawn every 3 dB in a logarithmic scale. Signal contours have been darkened. The center contours correspond to ground clutter. (From Woodman RF. High altitude resolution stratospheric measurements with the Arecibo 430-MHz radar. *Radio Science* 15(2): 417–422, March–April 1980. Copyright (1980) American Geophysical Union. Reproduced by permission of American Geophysical Union.)

directions one could determine the full velocity vector of the medium, including the vertical component, provided that the three scattering volumes are close enough to sample the same velocity field.

The MST (or ST) technique is the only technique capable of measuring directly the very small vertical component of the atmospheric motions. Accuracies of the order of a few centimeters per second are obtained for the on-line-of-sight velocities with only a minute of integration. Another important advantage of the technique is its high temporal resolution and continuity of observation. The time dependence of full vector velocity fields can be obtained showing the fastest temporal fluctuations of buoyancy waves at and below Brünt–Väissälä periods as well as the longest planetary wave periods, and beyond.

As far as the horizontal components of the wind are concerned, there are a variety of radiowave techniques that can be employed. At least half a dozen different acronyms have been coined for these methods, but in reality they are based on only two different principles. Some can be grouped as techniques based on multiple projections of the Doppler shift, as described above. The others are based on the relationship between the velocity of the diffraction pattern cast on the ground by the scattered EM field. These are measured by three or more non-collinear spaced antennas, that respond to the horizontal velocity of the medium responsible for the scattering. **Figure 5** depicts velocity parameters obtained with a BLR using this latter technique. Another technique belonging to the second group is the interferometric technique. Here antenna signals are processed in pairs. The cross-spectral correlation of these two received signals gives additional information, including the angle of arrival of the echo its angular velocity and the angular spread of the scattering region. But even this grouping is artificial, since it can be shown that the angular distribution of the scattered waves (pointing techniques) and the spatial distribution of the field on the ground (spaced receiver techniques) form a spatial Fourier transform pair – i.e., they are not independent.

For the interpretation of the spectral width, it is convenient to think of the scattering signal as coming from different independent subvolumes of the total scattering volume. The size of the subvolumes should be much smaller than the total volume but slightly larger than the Bragg scattering wavelength. Each of the subvolumes will scatter with a Doppler shift corresponding to its radial velocity. If we assume the scattering properties of the medium to be homogeneous, the Doppler frequency spectral width would be a measure of the radial velocity distribution of the subvolumes. In a turbulent mixing model, the spectral width is then directly related to the variance of the

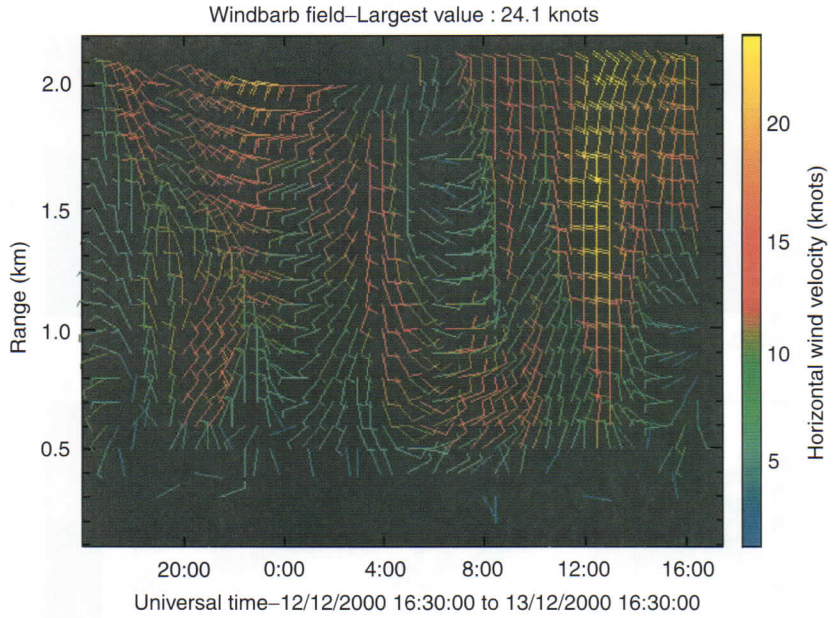

Figure 5 Windbarb velocity field as a function of altitude and time obtained with a VHF boundary layer radar. The vertical component corresponds to the NS component of the wind, and the horizontal to the EW component of the same. (Courtesy of the Atmospheric Physics group at the University of Adelaide.)

turbulent velocities and hence a measure of the turbulent kinetic energy and, through turbulence theory, is related also to the turbulence dissipation rate. **Figure 6** shows an experimental example of the three spectral moments, including the spectral width, as a function of altitude and time obtained by the ALWIN radar, in Andenes, Norway. In this case, they correspond to PMSE echoes.

The validity of the above interpretation of the spectral width depends on the validity of some implicit assumptions. We have implicitly assumed that the subvolumes have a frozen structure. In reality there are smaller-scale motions within the subvolume, even smaller than a wavelength. The measured spectrum is actually the convolution of the velocity distribution of this smaller structure with the distribution of the subvolume velocities. This assumption has no practical consequence, since the variance of the larger structures is much larger than that of the smaller scales and, in any case, the measured spectra actually include the contributions of the smaller scales.

We have also implicitly assumed that the average radial velocities of the subvolumes are all the same and that the mean Doppler shift is a measure of it. In practice the antennas have a finite beam width and the horizontal component of the wind will project different average values depending on the pointing angle to the subvolume with respect to the center pointing direction of the antenna. This effect can be very important, considering that the horizontal velocities are very large, of the order of tens of meters per second, while the turbulent velocities are only of the order of $10\,\mathrm{cm\,s^{-1}}$. The effect is known as the beam broadening effect. Fortunately, unless the beam width is of the order of ten degrees or more, the beam broadening effect can be corrected by deconvolving the spectrum with the known beam broadening effect. To do this one needs to know the horizontal velocity, which is measured by the technique.

Other sources of spectral broadening are the existence of shear and gravity waves. Shear is important only in oblique pointing directions when the altitude resolution is not capable of resolving the existence of a shear in the horizontal velocity (see for instance the spectrum at 15.2 km in **Figure 4**). In this case, the subvolume average radial velocities have systematic contributions from the different horizontal velocities at different altitudes. On the other hand, if there is a concurrent vertical pointing beam, shear broadening can be used to infer the value of the very same shear that produced it, even when the instrument is not capable of resolving it. Gravity waves can also contribute to the broadening, but only when the spectra have been obtained with an integration time that is longer than a significant fraction of the shortest (Brünt–Väissälä) periods in the wind fluctuations.

We have mentioned that acoustic wave density fluctuations are also capable of producing EM wave scattering. In this case the Doppler shift is given by the acoustic velocity and hence it can be used to determine

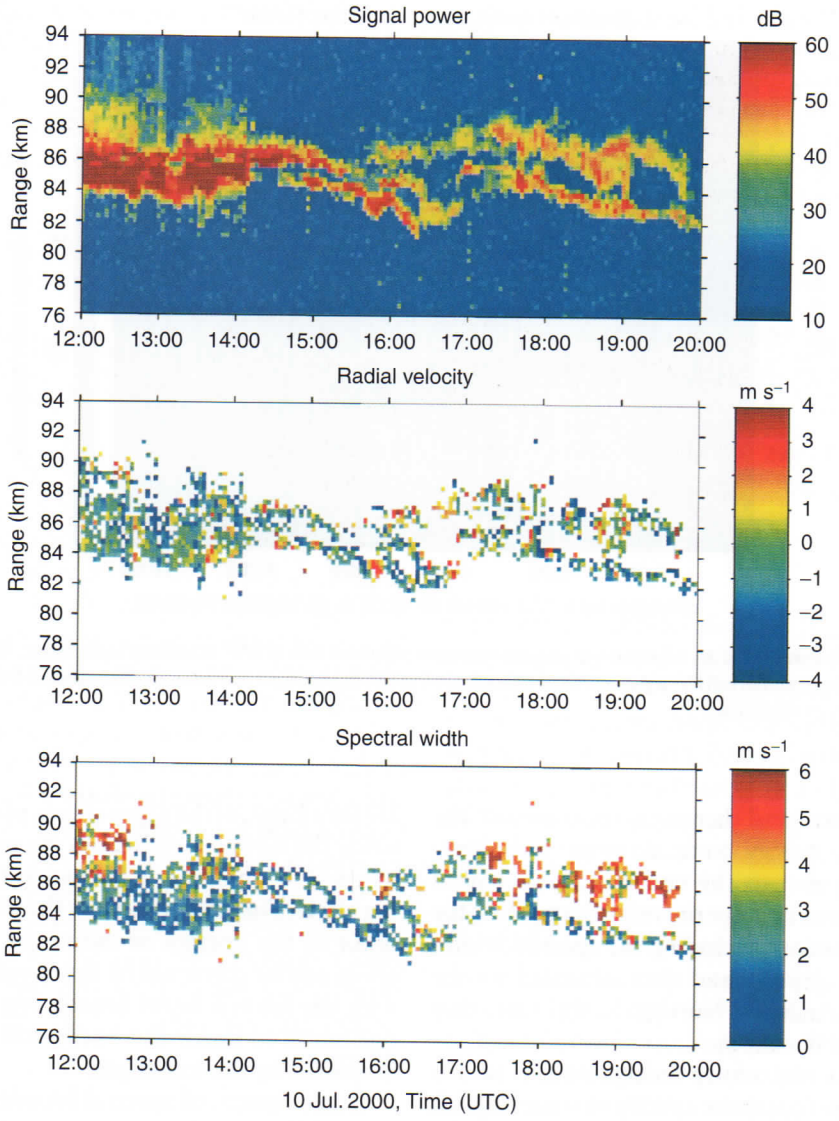

Figure 6 Colour shade display of the power, radial velocity, and spectral width of polar mesospheric summer echoes (PMSE) obtained with the ALWIN radar in Andenes, Norway. (Courtesy of the Institute for Atmospheric Physics, Kühlungsborn, Germany.)

the temperature of the medium, but the natural background level of the fluctuations is too weak to be of practical use: therefore artificial excitation of the waves by acoustic sources is necessary. The technique has been used successfully to measure tropospheric temperature profiles and is known as the radio acoustic sounding system (RASS).

See also

Boundary Layers: Neutrally Stratified Boundary Layer. **Clear Air Turbulence**. **Data Analysis:** Time Series Analysis. **Dynamic Meteorology:** Overview. **General Circulation:** Overview. **Mesosphere:** Polar Summer Mesopause. **Radar:** Doppler Radar; Incoherent Scatter Radar; Precipitation Radar.

Further Reading

Balsley BB (1981) The MST technique – a brief review. *Journal of Atmospheric and Terrestrial Physics* 43: 495–509.

Cho JYN and Röttger J (1997) An updated review of polar mesosphere summer echoes: observations, theory, and their relationship to noctilucent clouds and sub-visible aerosols. *Journal of Geophysical Research* 102: 2001–2020.

Gage KS (1990) Radar observations of the free atmosphere structure and dynamics. In: Atlas D (ed.) *Radar in Meteorology*, pp. 534–565. Boston, MA: American Meteorological Society.

Hocking WK (1997) Recent advances in radar instrumentation and techniques for studies of the mesosphere, stratosphere, and troposphere. *Radio Science* 32: 2241–2270.

Röttger J (1991) MST radar and incoherent scatter radar contributions to studying the middle atmosphere. *Journal of Geomagnetism and Geoelectricity* 43: 563–596.

Röttger J and Larsen MF (1990) UHF/VHF radar techniques for atmospheric research and wind profiler applications. In: Atlas D (ed.) *Radar in Meteorology*, pp. 253–281. Boston, MA: American Meteorological Society.

Woodman RF (1991) A general statistical instrument theory of atmospheric and ionospheric radars. *Journal of Geophysical Research* 96: 7911–7928.

Woodman RF and Guillen A (1974) Radar observations of winds and turbulence in the stratosphere and mesosphere. *Journal of the Atmospheric Sciences* 31: 493–505.

Precipitation Radar

S E Yuter, University of Washington, Seattle, WA, USA

Introduction

Precipitation radars are widely used to determine the location, size, and intensity of precipitating storms. Ground-based scanning precipitation radars are used in short-term weather and flood forecasting, and to estimate the distribution and amount of cumulative rainfall over a region. The weather services of many industrial countries have networks of operational radars that monitor precipitation near population centers. The output from these operational radar networks can be combined to provide a picture of the distribution of precipitation over synoptic-scale regions. Mobile precipitation radar on aircraft provides pilots with information to navigate safely around dangerous regions of hail and turbulence. Precipitation radars are also used to map the three-dimensional structure of storms. Spaceborne precipitation radar on low-orbit satellite maps the structure and distribution of precipitation around the globe over periods of months and years.

The British and Americans first developed weather radar during World War II. The precipitation radar transmits a pulse of electromagnetic energy via an antenna. When the transmitted energy encounters a reflector, such as a raindrop, part of the transmitted energy is scattered back toward the antenna, where it is received and amplified. The time delay between the original pulse transmission and the receipt of the backscattered energy is used to deduce the distance to the reflector. The relationship between the range-corrected, backscattered, returned power and the size and number of the reflecting targets is the physical foundation for interpreting precipitation radar data.

The frequency of electromagnetic waves f in Hz (s^{-1}) is defined as $f = c/\lambda$, where c is the speed of light and λ is the wavelength. Radar frequencies are divided into several bands, as shown in **Table 1**. The choice of frequency for precipitation radar is a tradeoff between the practical constraints of size, weight, cost, and the relation between the wavelength and the size of the target hydrometeors. Theoretical considerations favor the choice of the longer S-band and C-band wavelengths for many precipitation applications. However, use of these longer wavelengths is not always practical. The beam width for circular antennas is proportional to λ/d, where d is the antenna diameter. In comparison to shorter wavelengths, longer wavelengths necessitate a larger antenna to obtain a focused beam of the same angular beam width. Larger antennas are heavier, require more powerful motors to rotate them, and are more expensive than smaller antennas. Shorter X-, K_u-, and K_a-band wavelengths are often utilized in mobile precipitation radars deployed on spacecraft, aircraft, and ships where size and weight are more constrained as compared to stationary ground-based radars.

Table 1 Precipitation radar frequencies and wavelengths (adapted from Skolnik, 1990, and Rinehart, 1991)

Band designation	*Nominal frequency (GHz)*	*Nominal wavelength (cm)*	*Applications*
S	2–4	15–8	Surface-based radars
C	4–8	8–4	Mobile and surface-based radars
X	8–12	4–2.5	Mobile and surface-based radars
K_u	12–18	2.5–1.7	Mobile and spaceborne radars
K_a	27–40	1.1–0.75	Mobile and spaceborne radars

Precipitation Radar Components

The precipitation radar consists of a transmitter, receiver, transmit/receive switch, antenna, and display (**Figure 1**). In this simplified diagram, the processing of the electromagnetic signals into output suitable for display is included in the display block. A phase detector may be included to measure Doppler velocity. The radar transmitter contains a modulator that switches the transmitter on and off to form discrete pulses. The radar sends out a pulse and then switches to the receiver to listen. The range to the targets is obtained by comparing the time of pulse transmission to the time the backscattered pulse is received. In precipitation radars, the pulses are transmitted at a pulse repetition frequency (PRF) of $\sim$ 300–1300 Hz and each pulse is order 1 μs (10^{-6} s) in duration. The time between transmitted pulses limits the maximum range (r_{max}) the electromagnetic pulse can travel before the next pulse is transmitted (eqn [1])

$$r_{max} = \frac{c}{2PRF} \qquad [1]$$

The receiver detects and amplifies the received signals and averages the characteristics of the returned pulses over defined time periods. Typical peak transmitted power for an operational precipitation radar is 10^5–10^6 W. Typical received power is 10^{-10} W. The transmit/receive switch protects the sensitive receiver from the powerful transmitter. Without the switch, the radar transmitter would burn out the receiver. In practice, the transmit/receive switch is not perfect and a small amount of transmitted energy leaks into the receiver.

Radar antennas focus transmitted energy and direct it along a narrow angular beam. For scanning radars, this direction is often described in terms of an elevation angle relative to the ground and an azimuth angle relative to north. Moving the antenna points the axis of the beam in different directions, and permits scanning of two- and three-dimensional regions of the atmosphere. The antenna shape determines the radar beam size and shape. The radar energy is maximum along the center of the beam and decreases outward with increasing angular width. The beam width is defined as the angular width where the power is exactly half the maximum power. Most precipitation radars utilize a circular parabolic antenna for both transmission and reception.

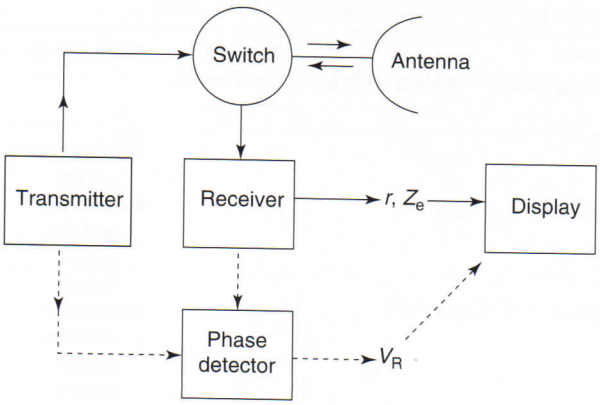

Figure 1 Simplified hardware block diagram of a precipitation radar. The non-Doppler portion of the system yields the range r and equivalent reflectivity factor (Z_e) of the target. Dashed lines connect parts of the system included in a Doppler radar that additionally measures the radial velocity of the target (V_r). (Adapted from Houze, 1993.)

The main purpose of the display is to distinguish scatterers at different ranges. A basic scanning radar display will usually indicate the compass angle and range to the radar echo in polar coordinates. **Figure 2** shows the range-corrected received power as a function of range along a single pointing direction of the antenna. This example illustrates that not all the energy received at the radar is backscattered from meteorological targets. Transmitter leakage and ground clutter from nearby nonmeteorological targets such as trees and buildings are present at close ranges in the display. The signal from a point target such as a radio tower is present at 50 km range. The wider signal associated with meteorological echo is present in the range between 90 and 115 km.

The Radar Equation

The radar equation expresses the relationship between the transmitted power and backscattered received power from precipitation targets in terms of the radar's hardware characteristics and the distance between the transmitter and the target. In this section, the radar equation and radar reflectivity will be derived by first making some simplifying assumptions and then gradually refining the terms to more accurately represent the electromagnetic theory underpinning precipitation radars.

Isolated Scatterers

The amount of power incident (P_i) at an isotropic target of cross-sectional area A_t at range r_1 from an isotropic transmitter is given by eqn [2], in which P_t is the transmitted power (**Figure 3A**).

$$P_i = \frac{P_t A_t}{4\pi r_1^2} \qquad [2]$$

Transmitted power and received power are commonly expressed in units of watts or dBm. The latter represents the ratio of power (P) in watts relative to 1 milliwatt ($10 \log_{10} [P/10^{-3}\,\text{W}]$). In a typical